Quantum heat transfer in harmonic chains with self-consistent reservoirs: Exact numerical simulations

Malay Bandyopadhyay and Dvira Segal
Chemical Physics Theory Group, Department of Chemistry University of Toronto, 80 St. George Street, Toronto, Ontario, M5S 3H6, Canada
(Received 10 June 2011; published 29 July 2011)

We describe a numerical scheme for exactly simulating the heat current behavior in a quantum harmonic chain with self-consistent reservoirs. Numerically exact results are compared to classical simulations and to the quantum behavior under the linear-response approximation. In the classical limit or for small temperature biases our results coincide with previous calculations. At large bias and for low temperatures the quantum dynamics of the system fundamentally differs from the close-to-equilibrium behavior, revealing in particular the effect of thermal rectification for asymmetric chains. Since this effect is absent in the classical analog of our model, we conclude that in the quantum model studied here thermal rectification is a purely quantum phenomenon, rooted in the quantum statistics.

DOI: 10.1103/PhysRevE.84.011151 PACS number(s): 05.60.Gg, 02.70.−c, 63.22.−m, 44.10.+i

I. INTRODUCTION

Understanding the role of quantum effects in the thermal-conduction properties of interacting systems is a challenging task. While in the classical regime molecular dynamic simulations provide a flexible tool for including anharmonic interactions to all orders [1,2], in the quantum limit treatments are typically limited to particular parameter domains [3]. Among the methods developed for tracking the quantum behavior of anharmonic systems we recall the nonequilibrium Green's function technique, which is perturbative in the nonlinear interaction strength [4,5], and the master equation approach, which is limited to models with weak-system bath couplings and to systems with few quantum states [6,7]. More recently, mixed classical-quantum molecular dynamics simulation tools were developed, valid at relatively high temperatures [8]. It was also demonstrated that a scheme based on the Born-Oppenheimer principle could be constructed in the context of thermal conduction, useful for studying the dynamics in the off-resonance regime [9]. Last, exact quantum simulations of the heat current characteristics can be performed for simplified models only [10].

In this paper we consider the problem of heat transfer in the quantum harmonic chain model with each inner site connected to a self-consistent (SC) reservoir. This model has been developed with the motivation to include nonlinear behavior in an effective way [2,11–13]. Specifically, here we would like to gain insight on the role of quantum effects at low temperatures on the thermal properties of one-dimensional (1D) chains. For brevity, we often refer to this model as the "SC model." It includes a linear chain of N beads connected to N independent thermal reservoirs, one at each site; see Fig. 1. While the temperatures of the reservoirs attached to the first and last particles impose the boundary conditions, the role of the inner (self-consistent) baths is to provide a simple scattering mechanism that might lead to local equilibration and to the onset of the (diffusional) Fourier's law of heat conduction [2,13]. In practice, the temperature of these $N-2$ internal baths is determined by demanding that in steady state, on average, there is no net heat flow between the chain atoms and these reservoirs.

The classical version of this model has been proposed in Refs. [11,12] and recently revisited in Refs. [13,14], demonstrating that for long chains Fourier's law is satisfied and a linear temperature profile is generated. It has been also proved that in the classical regime this model cannot support thermal rectification, an asymmetry of the current under the exchange of the temperature bias, even when some spatial asymmetry is provided [15,16]. The SC model is also of interest in the context of anharmonic lattices [17,18]. Overall, it is an example for a hybrid model, whose time evolution is dictated both by a Hamiltonian term (deterministic) and by stochastic effects.

The quantum analog of the SC model was studied by Visscher and Rich [19], who analyzed the limiting case of weak coupling to the SC reservoirs. The model was revisited by Roy and Dhar [20,21], who demonstrated that under the *linear response assumption* and for asymptotically long chains, Fourier's law holds and a temperature dependent thermal conductivity is realized. An analytical study of the SC model with alternate masses has revealed the role of quantum effects at low temperatures [22,23]. More recently, a mathematical analysis of the mass-graded SC model in the quantum domain has indicated the onset of thermal rectification, beyond the linear-response regime [24].

Focusing on the quantum SC harmonic chain model, one should note that exact analytic results are limited to the linear-response regime [20,21]. The reason is that beyond this limit, for large temperature biases, the self-consistent condition translates into a set of coupled *nonlinear* equations that seem intractable. Since an analytic solution is missing, in this paper we follow a numerical scheme for exactly simulating the transport properties of this model. The method is useful at low and high temperatures, in equilibrium, and for far-from equilibrium situations. It can be also applied onto three-dimensional systems. For simplicity, here we confine ourselves to 1D models. As an interesting application we perform numerical simulations on the SC harmonic chain model, incorporating a spatial asymmetry. In accordance with previous numerical and analytic indications [24,25], we confirm that the system rectifies heat in the quantum regime, beyond the linear response limit.

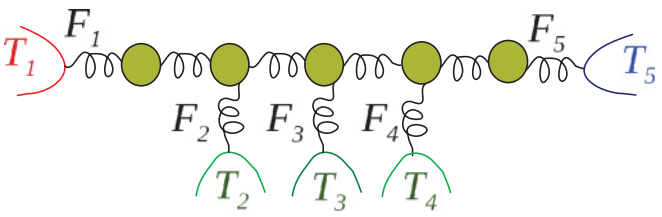

FIG. 1. (Color online) Scheme of a harmonic chain of $N = 5$ beads, where the inner particles are connected to SC baths. The wiggly lines represent harmonic bonds. The temperatures T_1 and T_5 set the boundary conditions; the temperatures T_l ($l = 2,3,4$) are determined by demanding that the leaking currents vanish, $F_l = 0$. The net heat current across the system is given by $F_1 = -F_5$.

The paper is organized as follows. In Sec. II we present the SC harmonic chain model and describe the numerical method. We further explain how to calculate the thermal properties of the model in the classical limit, and in the quantum regime, under the linear-response approximation. Section III provides some examples for the heat current characteristics in different domains, manifesting the onset of the thermal rectifying effect in an asymmetric setting. Section IV concludes.

II. MODEL AND METHOD

We now describe the SC model, introduced in Ref. [12]. The chain includes N atoms, where neighbors are connected by harmonic links. Each particle is also bilinearly (position-position) coupled to an independent thermal reservoir. The temperatures at the end points are set to T_1 and T_N, establishing the boundary conditions. In contrast, the temperatures of the internal reservoirs T_l ($l = 2,3,\ldots,N-1$) are determined in a self-consistent manner, by requiring that the net heat current flowing into or from the chain through each contact $l = 2,3,\ldots,N-1$ vanishes. For a schematic representation see Fig. 1.

The Hamiltonian of the chain H_S (system), its reservoirs H_{B_m} (baths), and the interaction term $\mathcal{V}_{B_m}$ is given as the sum of quadratic terms,

$$H = H_S + \sum_{m=1}^{N} H_{B_m} + \sum_{m=1}^{N} \mathcal{V}_{B_m}, \tag{1}$$

where

$$\begin{aligned} H_S &= \tfrac{1}{2}\dot{X}_S^T M_S \dot{X}_S + \tfrac{1}{2} X_S^T \Phi_S X_S, \\ H_{B_m} &= \tfrac{1}{2}\dot{X}_{B_m}^T M_B \dot{X}_{B_m} + \tfrac{1}{2} X_{B_m}^T \Phi_{B_m} X_{B_m}, \\ \mathcal{V}_{B_m} &= X_S^T V_{B_m} X_{B_m}. \end{aligned} \tag{2}$$

Here M_S and M_B are real diagonal matrices representing the masses of the particles in the chain and the bath particles, respectively. The quadratic potential energies for the chain and baths are given by the real symmetric matrices Φ_S and Φ_{B_m}, respectively. The term V_{B_m} denotes the interaction between the chain and the mth bath. The column vectors X_S and X_{B_m} are the Heisenberg operators of the particle displacements about some equilibrium configuration. In particular, $X_S = \{X_1, X_2, \ldots, X_N\}$ with X_m as the position operator of the mth particle of the chain. The momentum operators are given by $\dot{X} = M^{-1}P$, where $\{X_m, P_m\}$ satisfies the usual commutation relation, $[X_l, P_m] = i\hbar\delta_{l,m}$.

Since the system is entirely harmonic, a generalized Langevin equation for the system displacements can be written [2,20,26]. This is done by formally solving the Heisenberg equations of motion (EOM) for the bath operators, then plugging them into the EOM of the system displacements. In the ohmic limit this results in

$$M_l \ddot{X}_l = -(2X_l - X_{l-1} - X_{l+1}) - \gamma_l \dot{X}_l + \eta_l \tag{3}$$

for each bead. Here M_l is the mass of the lth particle, and the force constants are taken as unity. The chain-bath coupling strengths are enclosed within the friction coefficients γ_l. The noise-noise correlations, in frequency domain, satisfy

$$\begin{aligned} &\frac{1}{2}\langle \eta_l(\omega)\eta_m(\omega') + \eta_l(\omega')\eta_m(\omega)\rangle \\ &\quad = \frac{\gamma_l \omega}{2\pi} \coth\left(\frac{\omega}{2T_l}\right)\delta(\omega+\omega')\delta_{l,m}. \end{aligned} \tag{4}$$

The steady-state heat current can be obtained by evaluating (two-point) position-momentum correlation functions [20]. Specifically, it can be shown that the heat current from the lth reservoir into the chain is given by

$$\begin{aligned} F_l = \sum_{m=1}^{N} \gamma_l \gamma_m \int_{-\infty}^{\infty} d\omega \omega^2 |[G(\omega)]_{l,m}|^2 \frac{\omega}{\pi} \\ \times [f(\omega, T_l) - f(\omega, T_m)]. \end{aligned} \tag{5}$$

Here the matrix G is the inverse of a tridiagonal matrix with off-diagonal elements equal to -1 and diagonal elements $2 - M_l\omega^2 - i\gamma_l\omega$, $f(\omega,T) = [e^{\omega/T} - 1]^{-1}$ denotes the Bose-Einstein distribution. The temperature profile across the system is obtained by *demanding* that

$$F_l = 0, \quad l = 2,3,\ldots,N-1. \tag{6}$$

This condition translates into a set of $N-2$ nonlinear equations, yielding the inner baths' temperatures T_l. Plugging the resulting temperatures inside the expression for F_1 (or equivalently inside F_N) yields the steady-state net heat current flowing across the system,

$$J = F_1 = -F_N. \tag{7}$$

An exact-analytic solution of Eq. (6) is generally not accessible. A mathematical analysis has been carried out only perturbatively for a specific model with $N = 3$ [24]. In the linear response regime (or in the classical limit) these $N-2$ equations reduce into a set of *linear* equations, which can be readily solved as we explain below. Here, with the motivation to treat quantum systems beyond linear response, we follow an iterative numerical scheme for acquiring the exact solution of Eq. (6), i.e., the set of the inner-baths temperatures.

A. Quantum case: Exact simulations

The root of Eq. (6) can be standardly obtained using the powerful Newton-Raphson (NR) method [27]. This scheme proceeds as follows: Given a well-behaved function $f(x)$, a

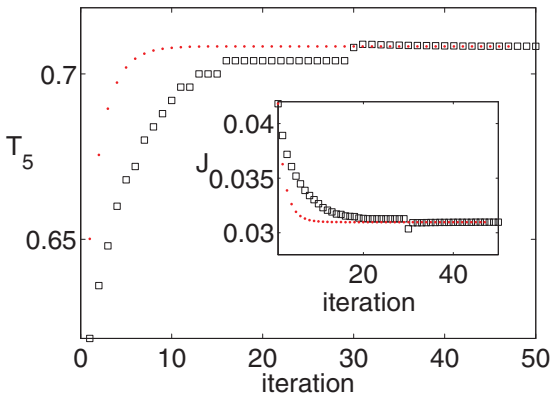

FIG. 2. (Color online) Convergence of the inner reservoirs' temperatures with increasing number of iterations. $N = 10$, $\beta_1 = 1$, $\beta_N = 5$, and $\gamma_n = 0.2$ for $n = 1, \ldots, N$. The main plot shows the temperature at site number 5. The inset displays the corresponding convergence of the net heat current, F_1. Results are obtained using the numerical method (12) (square) and the Newton-Raphson method (dotted).

good estimate for the root r, $f(r) = 0$, is reached by iteratively solving

$$x_{k+1} = x_k - \frac{f(x_k)}{f'(x_k)}, \tag{8}$$

with x_0 as the initial guess and $f'(x)$ the first derivative at the point x. In the present case we deal with a multivariable $(N-2)$ system; thus at each iteration k we correct the temperature of each internal site l using

$$T_l^{(k+1)} = T_l^{(k)} - \sum_{p=2}^{N-1} (D^{-1})_{l,p} F_p\left(T_n^{(k)}\right). \tag{9}$$

Here $T_n^{(k)}$ denotes the temperature profile $(n = 1, \ldots, N)$ after the kth iteration; the initial guess for the profile is, e.g., the average temperature in the system. The matrix D is the Jacobian matrix, $D_{i,j} = \partial F_i / \partial T_j$. It is evaluated using an analytic formula at the temperature profile obtained at the kth iteration. While convergence here is relatively fast (Fig. 2) the algorithm requires adjustments once some of the internal friction terms vanish (i.e., the corresponding SC reservoirs are turned off) to avoid divergencies. We thus describe next a more flexible, yet direct technique. It can be used even when some of the SC baths are disconnected without any adjustments. This method is more expensive than the NR technique since it relies on the construction of a temperature grid about each site. We verified that results from both methods coincide. We also found that ∼20–50 iterations were required to achieve convergence using either tools, depending on the chain size and temperatures. A demonstration of the method convergence follows its presentation.

We now present our plain approach for solving the nonlinear equations (6), valid with and without SC baths. We rearrange the expression for F_l [Eq. (5)] as follows:

$$\sum_{m=1}^{N} S_{l,m}(T_l) = \sum_{m=1}^{N} S_{l,m}(T_m), \tag{10}$$

where

$$S_{l,m}(T) = \gamma_l \gamma_m \int_{-\infty}^{\infty} d\omega \omega^2 |[G(\omega)]_{l,m}|^2 \frac{\omega}{\pi} f(\omega, T). \tag{11}$$

Given T_1 and T_N, our goal is to obtain the temperatures of the SC baths T_l $(l = 2, \ldots, N-1)$. This can be done by following an iterative procedure. We first make an initial guess for the temperature profile $T_l^{(0)}$. For example, we pick the average temperature $T_l^{(0)} = (T_1 + T_N)/2$. These values are inserted into the *right-hand side* of Eq. (10). For each site, we then search for the value $T_l^{(1)}$ that yields an equality. We do it by calculating the *left-hand side* of Eq. (10) over a fine grid of temperatures, searching for the temperature $T_l^{(1)}$ that minimizes the difference $|\sum_{m=1}^{N} S_{l,m}(T_l^{(1)}) - \sum_{m=1}^{N} S_{l,m}(T_m^{(0)})|$. This process is repeated for each of the inner atoms, to obtain the set of corrected temperatures $T_l^{(1)}$. In the next iteration these temperatures are used as the basis supposition, for receiving the subsequent corrected profile $T_l^{(2)}$. Formally, at the kth step we solve the following equation $N-2$ times, for each inner site l,

$$\sum_{m=1}^{N} S_{l,m}\left(T_l^{(k+1)}\right) = \sum_{m=1}^{N} S_{l,m}\left(T_m^{(k)}\right). \tag{12}$$

The procedure is repeated until we converge the temperature profile T_l and the current F_1. In other words, we maintain their values through iterations. One should further verify that the currents F_l, $(l = 2, \ldots, N-1)$, flowing between the inner sites and the SC reservoirs, are negligible, as we explain next.

There are two main sources of error in our procedure: (1) The frequency integration in Eq. (11) is carried out numerically, by discretizing energies between a lower and upper cutoffs. Selecting a fine frequency step $\Delta\omega$ and a large energy cutoff $\omega_c \gg \omega_S$, with ω_S as the chain characteristic frequency, we have verified that our results are robust against $\Delta\omega$ and ω_c. (2) Equation (12) is solved on a discretized temperature grid. It is obvious that for a coarse grid the inner reservoirs' temperatures may significantly deviate from the exact SC values, and leakage occurs [28]. To control this error we choose a mesh fine enough such that $|F_l|/|F_1| < 10^{-4}$ for $l = 2, 3, \ldots, N-1$. In addition, since for long chains the overall-net energy exchange between the SC baths and the system may accumulate to large values, we also verify in our simulations that the incoming and outgoing fluxes, $|F_1|$ and $|F_N|$ (equal in principle), differ by less than 0.1%.

In practice, we found that delicate grids should be adopted for reaching a good accuracy for chains with $N \gtrsim 10$. We therefore developed a two-step procedure to improve efficiency. In the first step a relatively rough grid is constructed, $\delta T = (T_1 - T_N)/200$, and the iterative procedure Eq. (12) is followed to convergence, in the sense that the temperature profile stays fixed through iterations. However, these temperatures still deviate from the optimal (SC) temperatures, and significant leakage may take place. We denote by p the number of iterations in this part.

In the second step of our procedure an *individual* mesh is constructed at each site by dividing the sector $[T_l^{(p)} - \delta T, T_l^{(p)} + \delta T]$ into, e.g., 200 elements. Given these individualized grids, we iterate Eq. (12) q more times, to converge the

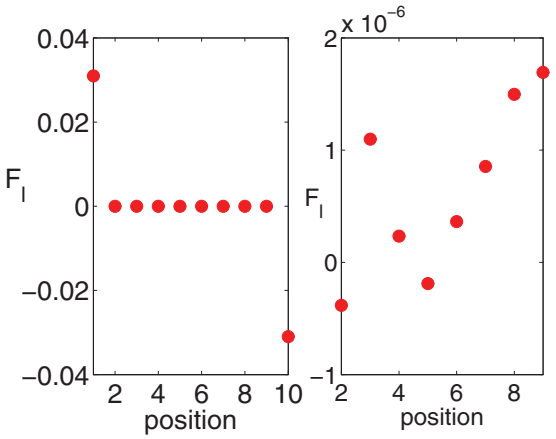

FIG. 3. (Color online) (left) The currents F_l, $l = 1,2,\ldots,N$ [see Eq. (5)], at each site, for a chain with $N = 10$ beads, obtained after applying the iterative procedure $p + q = 50$ times, $\beta_1 = 1$, $\beta_N = 5$, $\gamma_l = 0.2$. (right) Zooming on the internal currents F_2 to F_9, zero for perfect SC reservoirs.

temperature profile again. Overall, $p + q$ iterations are therefore performed, adopting a two-level grid. More generally, one could use a hierarchy of temperature grids, individually constructed around each particle for further improving the accuracy of the results and the method efficiency.

Figures 2 and 3 demonstrate the convergence of this scheme, as reflected in three quantities: (1) The temperature of each internal bath should not vary between iterations upon convergence. In conjunction, (2) the current flowing through the system (F_1) should remain fixed. (3) Net exchange of energy between the internal reservoirs and the chain should be rudimentary, relative to the current crossing the system. It is important to note that one can reach convergence with respect to the first two criteria, yet the reservoirs may not act as SC baths since the temperature grid selected is too rough.

For testing our method, we consider a uniform chain with $N = 10$ particles of unit mass. The friction is uniform along the chain, $\gamma_n = 0.2, n = 1,2,\ldots,N$. Figure 2 presents the temperature at the chain center (T_5) as we repeatedly solve Eq. (12). The small jump after 30 iterations arises due to the redefinition (and refinement) of the temperature grid at this point. The inset shows the (concurrent) convergence of the heat current $F_1 = -F_N$. A comparison to the Newton-Raphson method demonstrates that the NR method has superior convergence properties, starting at the same initial conditions, $T_l^{(0)} = T_a$ for the central beads.

We also verify that the reservoirs indeed behave as SC baths. Figure 3 displays the currents in the system, in particular the leakage currents $F_{l\neq 1,N}$ after 50 iterations. We confirm that the local leakage is smaller by four orders of magnitude than the net heat current F_1 (right panel). This assures us that at the end of the iterative procedure the reservoirs serve as SC baths.

B. Quantum linear-response regime and classical calculations

We outline here the process for obtaining the heat current behavior for the SC model in the quantum linear response regime or in the classical domain. In both cases Eq. (6) reduces into a set of linear equations.

In the quantum regime under the linear response approximation one assumes that temperature differences along the chain are small, $T_l - T_{l-1} \ll T_l$; thus the differences of Bose-Einstein functions $(f_l - f_m)$ in Eq. (5) can be replaced by the derivative $(T_l - T_m) \times \partial f/\partial T_a$ with $T_a = (T_1 + T_N)/2$. This approximation is valid close to equilibrium, for $|T_1 - T_N| \ll T_1, T_N$, or for very long chains with small local gradients. Under this approximation Eq. (5) reduces to

$$F_l = \sum_{m=1}^{N} \gamma_l \gamma_m \int_{-\infty}^{\infty} d\omega \omega^2 |[G(\omega)]_{l,m}|^2 \frac{\omega}{\pi} \times \frac{\omega}{4T_a^2} \mathrm{csch}^2\left(\frac{\omega}{2T_a}\right)(T_l - T_m). \quad (13)$$

Similarly, in the classical limit the quantum statistics is replaced by its high-temperature limit, $f(\omega,T) \sim T/\omega$, and Eq. (5) becomes

$$F_l = \sum_{m=1}^{N} \gamma_l \gamma_m \int_{-\infty}^{\infty} d\omega |[G(\omega)]_{l,m}|^2 \frac{\omega^2}{\pi}(T_l - T_m). \quad (14)$$

Equations (13) and (14) are both linear in the SC baths temperatures. Therefore, we can organize these equations as $F_l = \sum_m C_{l,m}(T_l - T_m)$, with $C_{l,m}$ containing the frequency integration. Demanding that $F_l = 0$ for l=2, ... ,$N - 1$, we get the exact solution [16]

$$\mathbf{T} = A^{-1} v. \quad (15)$$

Here A is a diagonal matrix with $N - 2$ rows for $l = 2,3,\ldots,N-1$. Its diagonal elements are $\sum_{m\neq l} C_{l,m}$, and the nondiagonal elements are given by $-C_{l,m}$. v is a vector defined as $v_l = C_{l,1}T_1 + C_{l,N}T_N$. The vector $\mathbf{T}$ includes the sought-after inner temperatures T_2 to T_{N-1}. Last, given the vector $\mathbf{T}$ the current F_1 can be readily calculated.

III. RESULTS

A. Quantum effects in thermal conduction

We recall that the self-consistent reservoirs were introduced as a tool to include in an effective way anharmonic processes. Our objective here is to demonstrate novelty in transport mechanisms in the deep quantum domain, beyond linear response, as a result of the introduction of these SC reservoirs. Furthermore, we compare simulations using the classical, quantum linear response, and quantum-exact treatments, unveiling the importance of quantum effects at low temperatures, for systems far from equilibrium. In the simulations reported here quantum results were obtained using the scheme described in Sec. II A. We refer to these calculations as "quantum exact" (QE). We used Eq. (13) to obtain data in the quantum domain under the linear response approximation, denoted by "quantum linear-response" (QLR). The classical (C) behavior was acquired using Eq. (14). The following parameters were typically used: unit masses and unit force constants [see Eq. (1)] and inverse temperatures $\beta \equiv 1/T$ ranging between $\beta \sim 0.1$–20. Within these parameters one expects to observe an effective classical behavior when $\beta \lesssim 0.2$. We also denote the average temperature by $T_a = (T_1 + T_N)/2$ and the overall bias by $\Delta T = T_1 - T_N$.

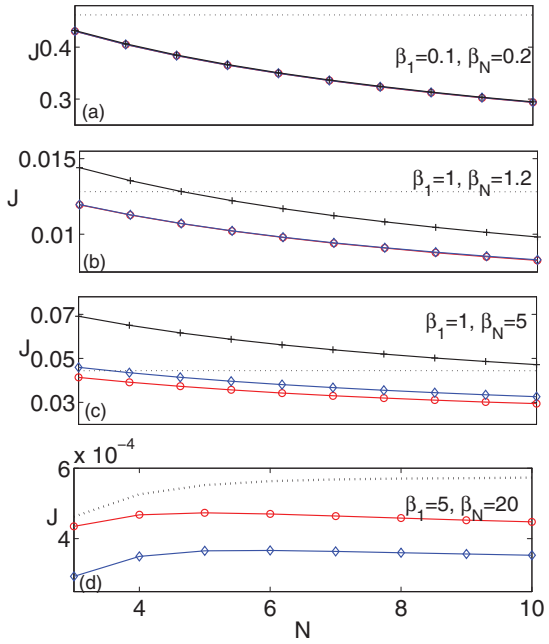

FIG. 4. (Color online) Heat current as a function of chain size using the quantum-exact method (○), quantum linear response formalism (diamond), and the classical limit (+). $\gamma_l = 0.2$ for all sites. (a) $\beta_1 = 0.1$, $\beta_N = 0.2$, (b) $\beta_1 = 1$, $\beta_N = 1.2$, (c) $\beta_1 = 1$, $\beta_N = 5$, (d) $\beta_1 = 5$, $\beta_N = 20$. The dotted lines represent the exact quantum behavior when the internal reservoirs are detached from the chain.

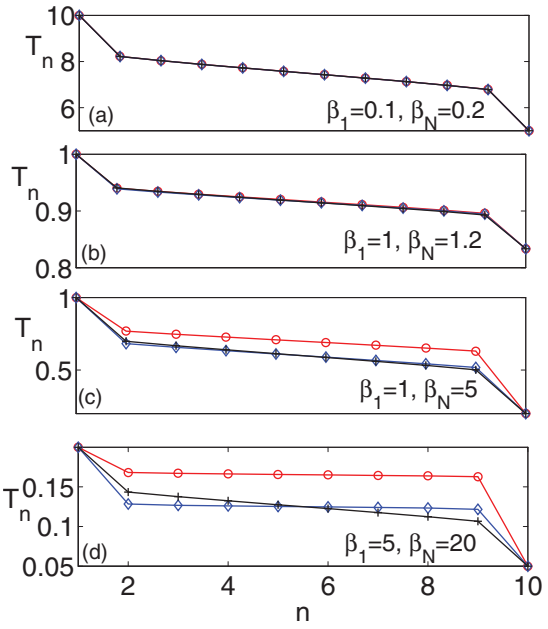

FIG. 5. (Color online) Temperature profile of the SC reservoirs at site n, $N = 10$, using the exact quantum method (○), quantum linear response formalism (diamond), and the classical expression (+), $\gamma_l = 0.2$ for all sites. (a) $\beta_1 = 0.1$, $\beta_N = 0.2$, (b) $\beta_1 = 1$, $\beta_N = 1.2$, (c) $\beta_1 = 1$, $\beta_N = 5$, (d) $\beta_1 = 5$, $\beta_N = 20$.

Figure 4 displays the heat current as a function of size for a uniform chain, comparing data attained from the three different methods: QE, QLR, and C. We analyze the behavior in four cases: (a) at high temperatures corresponding to the classical limit, (b) for intermediate temperatures $T_a \sim \omega_S$ and at small temperature bias $\Delta T < T_a$, corresponding to the linear-response regime (ω_S is a characteristic system frequency), (c) at low temperatures and for far-from equilibrium situations, $\Delta T/T_a \sim 1$, and (d) at very low temperatures, in the deep quantum regime $T_a \ll \omega_S$ and at large bias $\Delta T/T_a \sim 1$.

As expected, in the high-temperature regime the three methods yield the same value (a). At lower temperatures, yet adopting a small temperature difference, we find that QE and QLR calculations agree, while classical simulations overestimate the current (b). At low temperatures and large bias, panel (c) demonstrates that QLR calculations overestimate the exact value. In order to appreciate the role of the SC reservoirs, the dotted line further marks the value of the heat current, which is obtained within a full quantum calculations while nullifying the SC reservoirs. We find that in the absence of these reservoirs the current remains fixed. This is indeed the expected behavior for harmonic chains with a resonance thermal conduction mechanism, applicable at high temperatures [26].

Figure 4(d) exemplifies the heat current behavior at extremely low temperatures and for a large temperature bias, $\Delta T/T_a \sim 1$. Classical results (not shown) are higher by an order of magnitude than quantum data. The following observations can be made: (1) Within the QLR and QE methods, the current demonstrates an enhancement with size up to $N \sim 5$, followed by a decay. However, *in the absence* of the SC internal reservoirs (dotted line) the current systematically increases with size. This behavior could be reasoned as follows: With increasing chain length the low frequency modes of a periodic linear chain are down-shifted [26], eventually coming into resonance with the populated bath modes. This effect leads to the enhancement of the heat current with size: The behavior, indeed, is detected in the absence of the SC baths [26]. However, when the internal SC reservoirs are added, scattering mechanisms are responsible for an effective diffusional motion, resulting in the decay of the current with size [2]. The combination of these two trends produces the turnover of the current around $N \sim 5$. (2) In the deep quantum regime the QE current is higher that the QLR result, in contrast to the behavior observed in Fig. 4(c). As we show in Fig. 5(d), QLR calculations underestimate the factual temperature profile, in this case by about 30%. This fact can explain the similar deviation in the current. On the other hand, QLR calculations may produce a more significant temperature gradient within the chain; see, e.g., Fig. 5(c), resulting in currents larger than the QE data. As a result of these two counteracting factors, it is not trivial to predict *ad hoc* whether the accurate quantum result is above or below the QLR limit.

We now display the temperature profile for a chain with $N = 10$ particles. We calculate it using the three methods, QE, QLR, and C, in the four parameter domains mentioned above. Figure 5 shows that the three calculations generally agree at high temperatures and for $\Delta T/T_a \ll 1$. In contrast, at very low temperatures and for $\Delta T/T_a \sim 1$ the QE results deviate from the QLR and the classical data in a profound way. Specifically, for this (symmetric) setup QLR and classical calculations provide reservoirs temperatures that *symmetrically* vary around the average temperature $T_a = (T_1 + T_N)/2$ [16].

In contrast, QE calculations reveal that the chain temperature is actually *higher* than this temperature. This shifted profile stems from the nonlinear Bose-Einstein distribution function characterizing the reservoir statistics. It is also of interest to note that classical and QLR simulations generally predict an internal temperature gradient that is higher than the QE value. Specifically, with classical simulations we compute a local gradient that is larger by an order of magnitude from the QLR and the QE behavior [Fig. 5(d)]. This considerable disagreement reflects itself in the classical heat current, in this case high by one order of magnitude compared to the exact results.

B. Application: Quantum thermal rectification

Thermal rectification, an asymmetry of the heat current for forward and reversed temperature gradients, has been extensively analyzed in the last decade [29,30]. In a desirable rectifier the system behaves as an excellent heat conductor in one direction of the temperature bias, while for the opposite direction it effectively acts as an insulator. It is agreed that junctions incorporating anharmonic interactions with some sort of spatial asymmetry should exhibit this effect [29]. Since the SC model includes, in an effective way, anharmonic interactions through the action of the SC reservoirs, it is of interest to explore whether this model could demonstrate the rectifying effect when some spatial asymmetry is incorporated. This question is of particular interest since neither the classical SC model nor the QLR SC case can show thermal rectification, even when asymmetry is introduced [15,16,23]. In a recent paper analytical arguments were put forward, indicating that quantum SC systems should rectify heat [24]. Numerical simulations on a three-terminal nanojunction with structural asymmetry have further found this effect, referred to as "ballistic thermal rectification," using the nonequilibrium Green's function method [25]. In what follows we demonstrate that this effect indeed exists in asymmetric quantum harmonic systems with SC baths by solving exactly the set of nonlinear equations. We incorporate asymmetry either by using a mass-graded chain (Fig. 6) or by connecting a homogeneous chain asymmetrically to the reservoirs at the boundaries.

Figure 7 displays the absolute value of the heat current for forward (J_+) and reversed (J_-) temperature biases, studying a mass-graded system with $M_1 = 0.2$ and $M_l = M_1 + 0.2 \times (l-1)$, using the QE method. While at high temperatures and for $\Delta T \ll T_a$ the effect is negligible and $J_+ \sim J_-$, at low temperatures and for large bias J_+ and J_- evidently deviate, with the current being larger in the direction of *increasing* masses. We also find that the rectification ratio

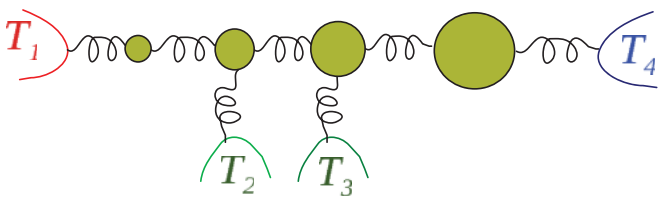

FIG. 6. (Color online) A scheme of the mass-graded harmonic chain with SC baths assuming $N = 4$ beads.

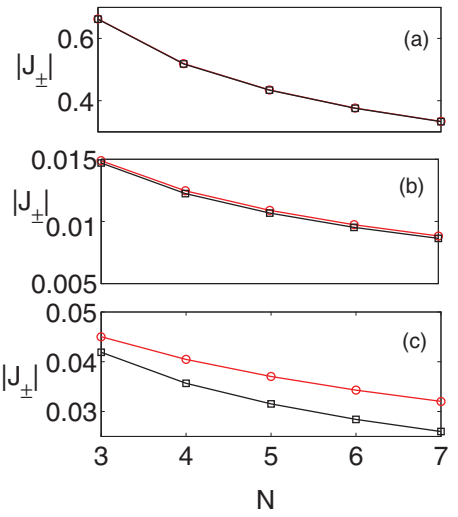

FIG. 7. (Color online) Thermal rectification in a mass graded system: The magnitude of the heat current as a function of chain size for forward temperature bias $T_1 > T_N$ (○) and for the backward direction, $T_N > T_1$ (square), $\gamma_n = 0.2$ for all sites, $M_1 = 0.2$, $M_n = M_1 + (n-1) \times 0.2$. In the forward direction we used (a) $\beta_1 = 0.1$, $\beta_N = 0.2$, (b) $\beta_1 = 1$, $\beta_N = 1.2$, and (c) $\beta_1 = 1$, $\beta_N = 5$. The opposite polarities were used in each case to generate J_-.

$|J_+/J_-|$ increases with chain size, an observation that can be reasoned by the growing mass ratio along the chain.

We note that in different experimental and theoretical studies, e.g., Refs. [30–33], the opposite tendency has been reported, and the preferred direction of heat transfer occurs from heavy to light atoms. It is obvious that the preferred direction depends on the details of the system studied [31–34]. For example, Ref. [32] reports on molecular dynamics simulations of heat conduction in mass-graded chains assuming anharmonic interactions between particles. The preferred heat transport direction in that model (heavy to light) is attributed to the vibrational coupling between low and high modes, arising due to anharmonicity in the system. The dynamics is further interpreted in terms of the overlap between the power

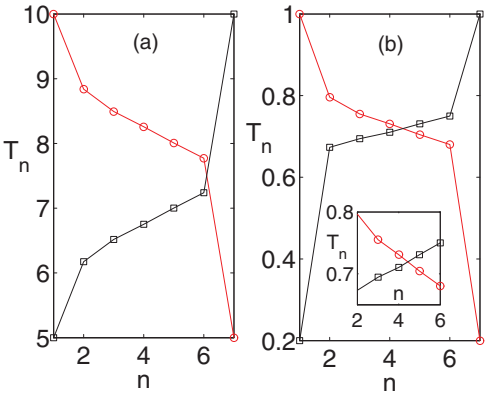

FIG. 8. (Color online) Temperature profile for a mass-graded $N = 7$ chain. In the forward direction (○) we used (a) $\beta_1 = 0.1$, $\beta_N = 0.2$ and (b) $\beta_1 = 1$, $\beta_N = 5$. The opposite polarities were used to generate the reversed profile (square). Other parameters are the same as in Fig. 7. The inset zooms on the chain center.

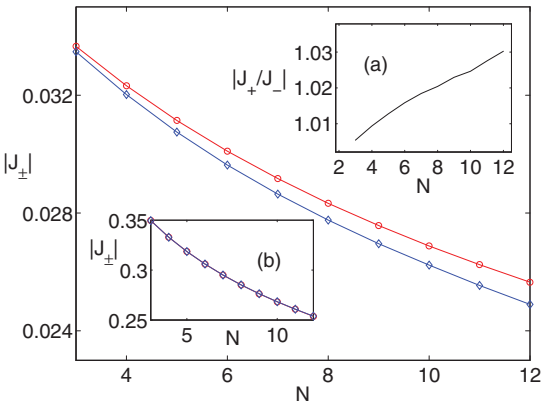

FIG. 9. (Color online) Thermal rectification in systems with contact asymmetry: The magnitude of the heat current as a function of chain size for forward temperate bias $T_1 > T_N$ (○) and for the backward direction, $T_N > T_1$ (diamond) $\gamma_1 = 0.1$, $\gamma_N = 0.4$, $\gamma_{n\neq 1,N} = 0.2$. $\beta_1 = 1, \beta_N = 5$, and the the reversed contact symmetry. (a) Rectification ratio $|J_+/J_-|$. (b) The forward and backward currents at high temperature $\beta_1 = 0.1$ and $\beta_N = 0.2$, and the reversed setup, with no significant rectification observed.

spectra at the chain ends. In contrast, simulations of thermal conduction in mass-graded nanotubes showed the opposite trend, explained by the transfer of vibrational energy from the transverse to the longitudinal direction [35,36].

In order to better understand the mechanism of thermal rectification in our model we display the temperature profile for the rectifying system in Fig. 8. At high temperatures [see Fig. 8(a)] there is a reflection symmetry with respect to the average temperature, when the temperature bias is reversed [16]. In contrast, in the quantum domain beyond linear response an asymmetry is discovered [Fig. 8(b)]: The *temperature gradient* at the chain center is larger when the light masses are in contact with the hot bath than the gradient generated in the reversed case. In particular, $\nabla T \sim -0.0230$ (-0.0185) when the heat flows in the direction of increasing (decreasing) masses weight. The ratio between these gradients indeed fits $|J_+/J_-|$ for $N = 7$; see Fig. 7(c). We emphasize that arguments based on the power spectra overlap [32,33] cannot be put on for the harmonic SC model since it does not include a physical mechanism for coupling different vibrational modes. This can be seen in Eq. (5): The heat current is retrieved by integrating over *separate* contributions, summing different frequency components.

One could also generate a spatial asymmetry in a mass-uniform SC model by coupling it unequally to the two ends, using $\gamma_1 \neq \gamma_N$. Since this is a contact asymmetry, one would generally expect its effect to diminish with size. Figure 9 still shows a small enhancement of the rectification strength with N, probably due to the increased importance of the scattering mechanisms (mimicking anharmonicity) with size.

Concluding this section, an interesting outcome of our study is the confirmation that the quantum harmonic chain with SC baths acts as a pure quantum thermal rectifier, since its classical analog, or the quantum model in the linear response regime, cannot demonstrate this effect [24]. This behavior is attributed to the introduction of the SC reservoirs, whose statistics at low temperatures is a *nonlinear* function of the local temperature, unlike the high-temperature or linear response behavior.

IV. SUMMARY

We presented a numerical method for acquiring the heat current and the temperature profile in the quantum harmonic chain model with SC reservoirs, beyond the linear response approximation. While the technique is generally valid for 3D models, we applied it here on 1D linear chains. At low temperatures and for large temperature biases we found that the exact quantum results significantly deviate from the QLR and classical behavior. As an application, we explored the thermal rectification effect in asymmetric systems, either by introducing mass asymmetry or by imposing a contact asymmetry. In both cases we concluded that quantum statistics is responsible for the onset of the nonlinear rectifying effect.

Our method could be generalized in two nontrivial ways. First, the scheme could be feasibly extended to describe non-Ohmic reservoirs, for studying the role of memory effects on thermal transport. This could be done by introducing frequency dependent friction terms in Eq. (5). Since the method is fully numerical, one can easily incorporate such frequency-dependent friction terms in the calculations. The second utility of the method is its application to fermionic systems. The analogous electronic model has been of extreme interest [37], where the SC reservoirs are interpreted as local dephasing probes [38]. For quantum systems, results were obtained only under the linear response assumption [39]. The principle introduced here could be easily modified, for treating the electronic problem, by replacing the bosonic distribution functions by fermionic functions, and by revising the equations as necessary. We expect that quantum effects will play a significant role at low temperatures and for large potential biases in the electronic case, similarly to the behavior found in the present phononic model.

To conclude, our calculations indicate that at low temperatures and for large biases the thermal conduction of SC quantum harmonic chains is fundamentally distinct from the linear response behavior or classical characteristics, manifesting interesting functionality that does not take place at high temperatures or close to equilibrium. It is of interest to extend our simulations and study longer chains, $N \sim 50$, for understanding the scaling of the heat current with size in the deep quantum domain and far from equilibrium.

ACKNOWLEDGMENT

The work was supported by an NSERC discovery grant.

[1] S. Lepri, R. Livi, and A. Politi, Phys. Rep. **377**, 1 (2003).
[2] A. Dhar, Adv. Phys. **57**, 457 (2008).
[3] J.-S. Wang, J. Wang, and J. T. Lü, Eur. Phys. J. B **62**, 381 (2008).
[4] N. Mingo and L. Yang, Phys. Rev. B **68**, 245406 (2003); N. Mingo, *ibid.* **74**, 125402 (2006); Therm. Nanosys. Nanomat. **118**, 63 (2009).

[5] J.-S. Wang, J. Wang, and N. Zeng, Phys. Rev. B **74**, 033408 (2006); J.-S. Wang, N. Zeng, J. Wang, and C. K. Gan, Phys. Rev. E **75**, 061128 (2007).
[6] D. Segal, Phys. Rev. B **73**, 205415 (2006).
[7] T. Ruokola and T. Ojanen, Phys. Rev. B **83**, 045417 (2011).
[8] J.-S. Wang, Phys. Rev. Lett. **99**, 160601 (2007).
[9] L.-A. Wu and D. Segal, Phys. Rev. E **83**, 051114 (2011).
[10] K. A. Velizhanin, H. Wang, and M. Thoss, Chem. Phys. Lett. **460**, 325 (2008); J. Chem Phys. **133**, 084503 (2010).
[11] M. Bolsterli, M. Rich, and W. M. Visscher, Phys. Rev. A **1**, 1086 (1970).
[12] M. Rich and W. M. Visscher, Phys. Rev. B **11**, 2164 (1975).
[13] F. Bonetto, J. L. Lebowitz, and J. Lukkarinen, J. Stat. Phys. **116**, 783 (2004).
[14] F. Barros, H. C. F. Lemos, and E. Pereira, Phys. Rev. E **74**, 052102 (2006).
[15] E. Pereira and H. C. F. Lemos, Phys. Rev. E **78**, 031108 (2008).
[16] D. Segal, Phys. Rev. E **79**, 012103 (2009).
[17] F. Bonetto, J. L. Lebowitz, J. Lukkarinen, and S. Olla, J. Stat. Phys. **134**, 1097 (2009).
[18] E. Pereira, Phys. Rev. E **82**, 040101(R) (2010).
[19] W. M. Visscher and M. Rich, Phys. Rev. A **12**, 675 (1975).
[20] A. Dhar and D. Roy, J. Stat. Phys. **125**, 801 (2006).
[21] D. Roy, Phys. Rev. E **77**, 062102 (2008).
[22] A. F. Neto, H. C. F. Lemos, and E. Pereira, Phys. Rev. E **76**, 031116 (2007).
[23] E. Pereira and H. C. F. Lemos, J. Phys. A: Math. Theor. **42**, 225006 (2009).
[24] E. Pereira, Phys. Lett. A **374**, 1933 (2010).
[25] L. Zhang, J.-S. Wang, and B. Li, Phys. Rev. B **81**, 100301(R) (2010).
[26] D. Segal, A. Nitzan, and P. Hänggi, J. Chem. Phys. **119**, 6840 (2004).
[27] W. H. Press, B. P. Flannery, S. A. Teukosky, and W. T. Vetterling, *Numerical Recipes in C: The Art of Scientific Computing* (Cambridge University Press, Cambridge, 1992).
[28] The central reservoirs, if not optimally tuned as SC baths, may either absorb or donate energy to the chain; see Fig. 3 showing internal currents with opposite signs. In the text we often refer to this net exchange of energy as "leakage."
[29] M. Terraneo, M. Peyrard, and G. Casati, Phys. Rev. Lett. **88**, 094302 (2002); B. Li, L. Wang, and G. Casati, *ibid.* **93**, 184301 (2004); D. Segal and A. Nitzan, *ibid.* **94**, 034301 (2005); B. Hu, L. Yang, and Y. Zhang, *ibid.* **97**, 124302 (2006); L. A. Wu and D. Segal, *ibid.* **102**, 095503 (2009); L.-A. Wu, C. X. Yu, and D. Segal, Phys. Rev. E **80**, 041103 (2009).
[30] C. W. Chang, D. Okawa, A. Majumdar, and A. Zettl, Science **314**, 1121 (2006).
[31] N. A. Roberts and D. G. Walker, Int. J. Therm. Sci. **50**, 648 (2011).
[32] N. Yang, N. Li, L. Wang, and B. Li, Phys. Rev. B **76**, 020301 (2007).
[33] N. Zeng and J.-S. Wang, Phys. Rev. B **78**, 024305 (2008).
[34] T. Hu, K. Hu, and Y. Tang, Physica B **405**, 4407 (2010).
[35] M. Alaghemandi, F. Leroy, E. Algaer, M. C. Böhm, and F. Müller-Plathe, Nanotech. **21**, 075704 (2010).
[36] M. Alaghemandi, F. Leroy, F. Müller-Plathe, and M. C. Böhm, Phys. Rev. B **81**, 125410 (2010).
[37] J. L. D'Amato and H. M. Pastawski, Phys. Rev. B **41**, 7411 (1990).
[38] M. Büttiker, Phys. Rev. B **33**, 3020 (1986).
[39] D. Roy and A. Dhar, Phys. Rev. B **75**, 195110 (2007).